Risk Analysis DOI: 10.1111/risa.12995

Human Dose–Response Data for *Francisella tularensis* and a Dose- and Time-Dependent Mathematical Model of Early-Phase Fever Associated with Tularemia After Inhalation Exposure

Gene McClellan,[1] Margaret Coleman,[2,*] David Crary,[1] Alec Thurman,[1] and Brandolyn Thran[3]

Military health risk assessors, medical planners, operational planners, and defense system developers require knowledge of human responses to doses of biothreat agents to support force health protection and chemical, biological, radiological, nuclear (CBRN) defense missions. This article reviews extensive data from 118 human volunteers administered aerosols of the bacterial agent *Francisella tularensis*, strain Schu S4, which causes tularemia. The data set includes incidence of early-phase febrile illness following administration of well-characterized inhaled doses of *F. tularensis*. Supplemental data on human body temperature profiles over time available from de-identified case reports is also presented. A unified, logically consistent model of early-phase febrile illness is described as a lognormal dose–response function for febrile illness linked with a stochastic time profile of fever. Three parameters are estimated from the human data to describe the time profile: incubation period or onset time for fever; rise time of fever; and near-maximum body temperature. Inhaled dose-dependence and variability are characterized for each of the three parameters. These parameters enable a stochastic model for the response of an exposed population through incorporation of individual-by-individual variability by drawing random samples from the statistical distributions of these three parameters for each individual. This model provides risk assessors and medical decisionmakers reliable representations of the predicted health impacts of early-phase febrile illness for as long as one week after aerosol exposures of human populations to *F. tularensis*.

KEY WORDS: Biothreat preparedness; dynamic modeling; patient stream simulation

1. INTRODUCTION

Tularemia, caused by the bacterial agent *Francisella tularensis*, is an endemic zoonotic disease reported in human and animal populations in the United States and around the world (World Health Organization, 2007). Aerosols of *F. tularensis* are of concern for medical personnel, laboratory workers (Barry, 2005; Burke, 1977; Centers for Disease Control & Prevention [CDC], 2017; Rusnak et al., 2004; U.S. Army Medical Research Institute of Infectious Diseases (USAMRIID), 2009, 2010), and for defensive preparedness planning for biological terrorism and biological warfare. The analysis and modeling presented in this article allow estimates of the patient stream to be expected as a function of time after exposure after an inhalation of *F. tularensis* resulting from a biological attack. A statistical description of

[1]Applied Research Associates, Inc., Arlington Division, Arlington, VA, USA.
[2]Coleman Scientific Consulting, Groton, NY, USA.
[3]Formerly U.S. Army Public Health Command, Environmental Health Risk Assessment Program, Aberdeen Proving Ground, MD, USA; now at Open-Gate Foundation, Elko, NV, USA.
[*]Address correspondence to Peg Coleman, Coleman Scientific Consulting, 434 West Groton Road, Groton, NY 13073, USA; peg@colemanscientific.org.

the onset of fever provides a prediction of the time distribution of patients seeking treatment in routine operations with no constraint on the availability of medical care. Similarly, a statistical description of how high the fever becomes, and how quickly without treatment, provides an estimate of the time distribution of operational casualties to be expected if medical care is limited or unavailable during combat operations. This article describes the development of the mathematical models from available data on human exposures and presents illustrative calculations for a company-sized unit.

1.1. *Francisella tularensis* and Human Tularemia

Tularemia has an extensive literature base summarized in excellent reviews (Adamovicz, Wargo, & Waag, 2006; Dembek, 2007; Dembek, Pavlin, & Kortepeter, 2007; Hepburn, Friedlander, & Dembek, 2007; Lyons & Wu, 2007; Sinclair, Boone, Greenberg, Keim, & Gerba, 2008). *F. tularensis* is thought to infect up to 250 animal hosts, which is more than any other known zoonotic pathogen (Dempsey et al., 2006). Early-phase tularemia manifests as febrile illness (fever and flu-like symptoms) and then can develop into several different forms (Dembek, 2007). The predominance of tularemia cases in humans reported worldwide are associated with arthropod vectors (ticks, mosquitoes, flies) or contact with infected small mammals (e.g., rabbits, hares, and voles). Most recorded cases are the glandular/ulceroglandular form of tularemia (World Health Organization, 2007). While tularemia after inhalation exposure is rare, it can occur after occupational exposures under specific conditions and is linked to the aerosolization of culture materials in laboratories. In addition, humans can be exposed to agricultural dusts contaminated by infected or dead animals (Dahlstrand, Ringertz, & Zetterberg, 1971; Halsted & Kulasinghe, 1978; Martone, Marshall, Kaufmann, Hobbs, & Levy, 1979; Sunderrajan, Hutton, & Marienfeld, 1985; Syrjälä, Kujala, Myllylä, & Salminen, 1985; Feldman et al., 2001; Eliasson et al., 2002; CDC, 2002; Hauri et al., 2010; Kaye, 2005; Shapiro & Schwartz, 2002; Simpson, 1929; Siret et al., 2005). Tularemia is highly infectious by inhalation; as few as 10–50 *F. tularensis* organisms are likely to cause febrile illness (Anno et al., 1998; Saslaw & Carhart, 1961). However, it is not communicable person to person, based on clinical and epidemiologic evidence (CDC, 2003; Dahlstrand et al., 1971; Eigelsbach, Saslaw, Tulis, & Hornick, 1968; Hepburn et al., 2007).

1.2. Documenting Fever as an Indicator of Illness and Performance Degradation

Early-phase tularemia is characterized by abrupt onset of febrile illness (sustained high fever within a day or so) that can be self-limiting and is rarely fatal with prompt medical care (Adamovicz et al., 2006; Dembek, 2007; Hepburn et al., 2007). Cases treated promptly with effective antibiotics typically became afebrile rapidly, for example, within 1–3 days of streptomycin treatment (Hughes, 1963; Martone et al., 1979; Overholt et al., 1961). For any of the forms of tularemia, systemic progression in the absence of prompt medical treatment can involve all the major organ systems, including the pulmonary system (Weinstein & Alibek, 2003). Virulence of *F. tularensis* is variable. Two of four *F. tularensis* subspecies (Type A, subspecies tularensis; and Type B, subspecies holarctica or paleoarctica) cause most human disease in the United States (CDC, 2003). The remaining two subspecies (novicida and mediasiatica) are infrequently associated with human disease. This study focuses on a virulent Type A strain of *F. tularensis* subsp. *tularensis* (Schu S4).

In the 1950s, high rates of laboratory-associated infections among workers handling *F. tularensis* cultures, despite repeated vaccinations (Eigelsbach, Tigertt, Saslaw, & McCrumb, 1962), prompted an extensive, multiyear, vaccine research program (Operation Whitecoat) carried out by U.S. Army scientists at Fort Detrick, Maryland. To date, only subsets of the human data generated are described in the peer-reviewed literature (Alluisi, Beisel, Bartelloni, & Coates, 1973; Hornick & Eigelsbach, 1966; Pekarek, Bostian, Bartelloni, Calia, & Beisel, 1969; Saslaw, Eigelsbach, Prior, Wilson, & Carhart, 1961; Sawyer, Dangerfield, Hogge, & Crozier, 1966; Shambaugh & Beisel, 1967) and these publications, as reports on prospective vaccine studies, focus primarily on vaccinated subjects with limited discussion of the unvaccinated controls.

More than two decades later, faced with a resurgent international threat of biological warfare, the Defense Nuclear Agency (DNA) initiated a retrospective study of the Operation Whitecoat data using de-identified clinical records obtained from the U.S. Army Medical Institute of Infectious Diseases (USAMRIID) at Fort Detrick, Maryland. The DNA research teams were led by Arthur P. Deverill and George H. Anno with assistance from former U.S. Army researchers Henry T. Eigelsbach and Harry G. Dangerfield. Access to clinical records was granted

for the retrospective biodefense study on febrile illnesses in unvaccinated volunteers administered aerosols of one of three agents causing treatable human fevers: tularemia caused by *F. tularensis*; Q fever caused by *Coxiella burnetii*; and staphylococcal entertoxin B (SEB) intoxication caused by *Staphylococcus aureus*. The primary purpose of the DNA study was to understand and quantify human vulnerability to bioagents of unvaccinated and untreated personnel and to predict the impact on military mission effectiveness via performance degradation associated with febrile illness. In 1996, DNA became the Defense Special Weapons Agency (DSWA). In 1998, a DSWA technical report including the data for Q fever and SEB, and a more detailed analysis of the data for tularemia, was published (Anno et al., 1998). For tularemia, the data for a total of 118 unique clinical records were compiled for volunteers inhaling doses ranging from 10 to 62,000 *F. tularensis* organisms (Anno et al., 1998). Clinical records for the other two febrile illnesses (Q fever and SEB intoxication) were also compiled and analyzed but are not summarized herein. Body temperature, severity of signs and symptoms, and performance degradation experienced by febrile volunteers were well correlated, and temporal profiles differed by agent/illness. In 1998, DSWA was merged into the Defense Threat Reduction Agency (DTRA).

The research effort reported by Anno et al. (1998) was closely coordinated by DTRA over the years with health care operations of the U.S. Army Office of the Surgeon General (OTSG). The refinements of the modeling for biological warfare agent effects are described in an OTSG report by Anno et al. (2005). The health effects models developed from these research efforts were utilized for casualty estimation to guide NATO medical planning (North Atlantic Treaty Organization, 2007). All results presented in this article are original in the sense that they have not previously been reported in the peer-reviewed literature. All results are either the work of the current authors or are drawn from the two Anno reports (Anno et al., 1998, 2005) for which one current author (GM) was also a co-author.

1.3. Modeling Dose- and Time-Dependence of Febrile Illness

Commanders and other decisionmakers require knowledge of dose- and time-dependencies for determining potential risk to health of military personnel and mission accomplishment over time after exposures to aerosols of *F. tularensis* and other agents. The data presented in this article were used to support a project at the Army Public Health Center to better understand the health effects of various inhaled doses to biological warfare agents in a military context. This article presents human dose–response data for tularemia by the inhalation route and describes the development of a model for early-phase tularemia. Disease incidence (probability of illness given dose) is modeled using the lognormal form of the simple probit model. The fever profile for early-phase febrile illness is characterized as illustrated in Fig. 1 using statistical distributions for three fever parameters (incubation period [IP] or time to onset of fever; near-maximum body temperature for early-phase illness; and rise time of temperature from onset to near-maximum). The use of Operation Whitecoat data to support stochastic simulation of affected personnel in a military unit after an attack with *F. tularensis* is illustrated in Fig. 2. The data (white boxes in the figure) for inhaled dose and the number of subjects with and without febrile illness determine a lognormal dose–response function, that is, a disease incidence model as indicated in the central gray box of the left-hand section of the figure. The fever data from those having febrile illness are used to determine three dose-dependent, statistical distributions of fever parameters as illustrated in the lower part of the right-hand section. These three models and the dose–response function (light gray boxes in the figure) enable a stochastic simulation of illness suffered by individuals in a unit exposed to *F. tularensis*

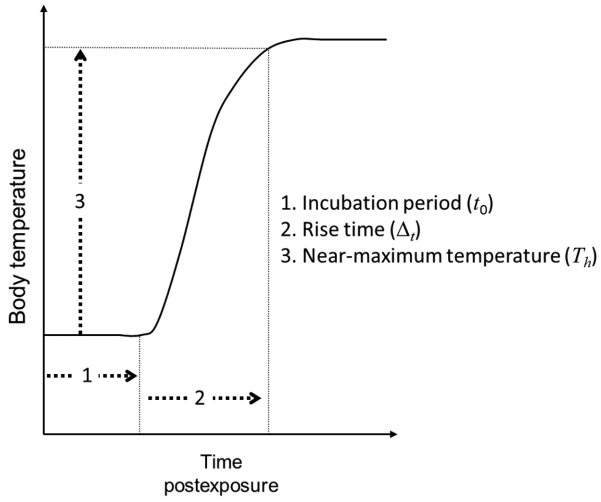

Fig. 1. Conceptual diagram for body temperature profile parameters in early-phase fever.

as indicated by the upper box in the right-hand section of the figure.

2. METHODS

This section describes the data analyzed and the mathematical methods used to develop a dose- and time-dependent mathematical model of early-phase fever associated with tularemia after inhalation exposure.

2.1. Human Dose–Response Data

The human data set includes 118 unvaccinated, healthy adult male volunteers from studies at Ohio State University (22 volunteers), University of Maryland (23 volunteers), and U.S. Army Medical Unit, Fort Detrick (73 volunteers) (Anno et al., 1998). Case reports include details of the signs and symptoms of illness recorded periodically after administration of known inhaled doses (dynamic aerosols of 1–5 μ diameter particles generated by nebulizer [modified Henderson-type apparatus using Collison spray] administered via tight-fitting mask). The criterion for determining a case of febrile illness was "observation of three or more sequential body [rectal] temperature measurements that met or exceeded 100 °F." For those who became ill, measurements continued approximately every six hours until recovery after antibiotic administration. Antibiotics were administered when fever plateaued at a high value after approximately 24 hours. Streptomycin or tetracycline was administered to halt disease progression and promote rapid and full recovery.

Of the 118 subjects exposed, 112 volunteers met the clinical case definition (see Table I). The frequency of signs and symptoms of febrile illness reported in the clinical records of these 112 subjects is illustrated in Fig 3. Fever is the single most comprehensive indicator of the degree of illness and subsequent degradation in performance (Anno et al., 1998, 2005). Fever profiles for the 112 volunteers with febrile illness are available in the clinical records with time-series data for body temperature recorded approximately every six hours starting at time of exposure. For the six volunteers who did not become ill, the temperature measurements continued for 10–12 days after exposure until the likelihood of illness had passed (Saslaw et al., 1961). These individuals were given terminal antibiotic therapy before discharge from the study (Saslaw et al., 1961). A typical temperature chart for a patient is illustrated in Fig. 4.

For each of the 112 febrile volunteers, parameters defining the fever profile are determined from the clinical charts. For the IP (onset time t_0 in days), the line connecting the nearest two points of the sequence of rising temperature measurements above normal is used to extrapolate for the time point of intersection with normal temperature, assumed to be 98.6 °F. Generally, these estimates of IPs describe the time at which the body temperature began to rise, then persisted above 100 °F for 18 hours. The

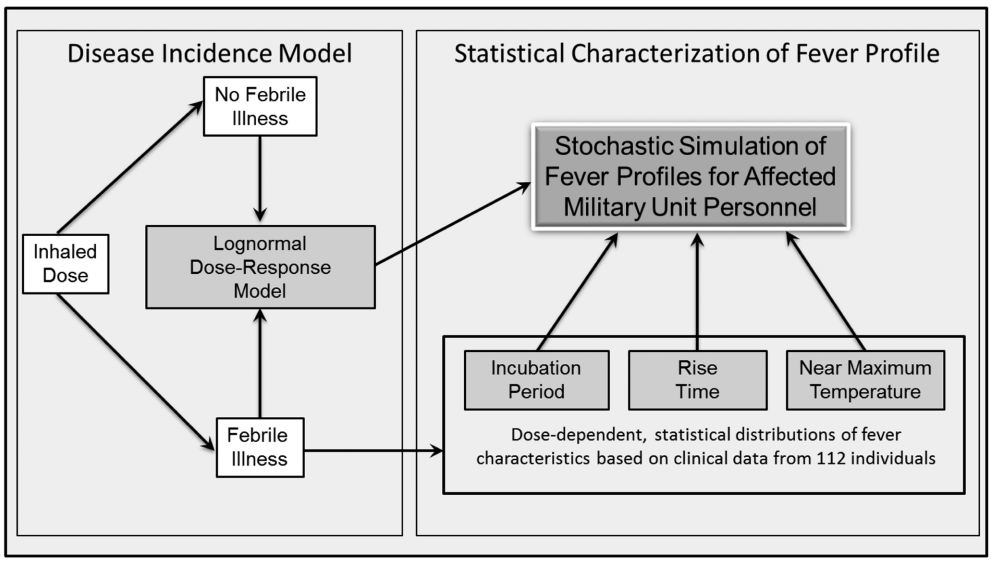

Fig. 2. Application of empirical data from Operation Whitecoat volunteers to stochastic simulation of military unit response to a bioattack.

Table I. Dose–Response Data Set for Early-Phase Febrile Illness

Volunteer Index	Estimated Individual Inhaled Dose (Organisms)	Febrile Illness	Volunteer Index	Estimated Individual Inhaled Dose (Organisms)	Febrile Illness	Volunteer Index	Estimated Individual Inhaled Dose (Organisms)	Febrile Illness	Volunteer Index	Estimated Individual Inhaled Dose (Organisms)	Febrile Illness
1	10	No	31	2,300	Yes	61	23,468	Yes	91	27,000	Yes
2	10	No	32	2,343	Yes	62	23,507	Yes	92	27,246	Yes
3	10	Yes	33	2,379	Yes	63	23,658	Yes	93	27,957	Yes
4	12	No	34	2,400	Yes	64	23,755	Yes	94	28,248	Yes
5	13	Yes	35	2,595	Yes	65	23,836	Yes	95	28,280	Yes
6	13	Yes	36	2,768	Yes	66	24,160	Yes	96	28,520	Yes
7	14	Yes	37	3,158	Yes	67	24,352	Yes	97	28,560	Yes
8	16	Yes	38	8,960	Yes	68	24,361	Yes	98	28,603	Yes
9	17	No	39	10,000	Yes	69	24,660	Yes	99	29,000	Yes
10	18	Yes	40	16,448	Yes	70	24,725	Yes	100	29,148	Yes
11	20	Yes	41	18,480	Yes	71	25,000	Yes	101	30,000	Yes
12	20	No	42	18,976	Yes	72	25,000	Yes	102	30,000	Yes
13	23	Yes	43	19,642	Yes	73	25,000	Yes	103	30,023	Yes
14	23	Yes	44	20,202	Yes	74	25,000	Yes	104	30,156	Yes
15	25	Yes	45	20,352	Yes	75	25,000	Yes	105	30,187	Yes
16	30	Yes	46	20,640	Yes	76	25,000	Yes	106	30,618	Yes
17	45	No	47	21,280	Yes	77	25,000	Yes	107	30,752	Yes
18	46	Yes	48	21,735	Yes	78	25,000	Yes	108	32,000	Yes
19	46	Yes	49	21,751	Yes	79	25,068	Yes	109	32,466	Yes
20	48	Yes	50	22,000	Yes	80	25,088	Yes	110	33,024	Yes
21	50	Yes	51	22,016	Yes	81	25,533	Yes	111	36,368	Yes
22	52	Yes	52	22,160	Yes	82	25,597	Yes	112	37,663	Yes
23	315	Yes	53	22,163	Yes	83	26,275	Yes	113	44,000	Yes
24	354	Yes	54	22,825	Yes	84	26,302	Yes	114	45,000	Yes
25	360	Yes	55	22,854	Yes	85	26,308	Yes	115	45,000	Yes
26	398	Yes	56	23,076	Yes	86	26,368	Yes	116	59,000	Yes
27	1,881	Yes	57	23,126	Yes	87	26,410	Yes	117	59,000	Yes
28	1,950	Yes	58	23,168	Yes	88	26,473	Yes	118	62,000	Yes
29	2,100	Yes	59	23,235	Yes	89	26,785	Yes			
30	2,253	Yes	60	23,396	Yes	90	26,987	Yes			

Note: Summarized from Anno et al. (1998). Data were collected at the U.S. Army Medical Unit, Ft. Detrick, or at Ohio State University or the University of Maryland in collaboration with Ft. Detrick researchers. Subsets of the data have been previously published (Alluisi et al., 1973; Hornick & Eigelsbach, 1966; Pekarek et al., 1969; Saslaw et al., 1961; Sawyer et al., 1966; Shambaugh & Beisel, 1967).

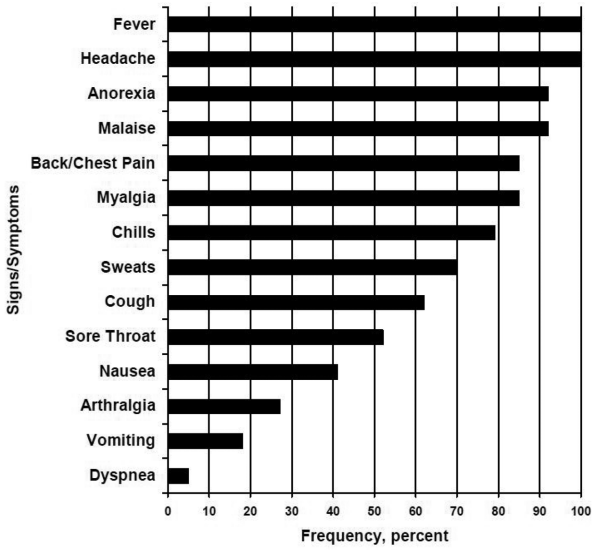

Fig. 3. Tularemia sign/symptom frequencies based on 112 unvaccinated subjects who developed fever after inhaled doses of *F. tularensis* strain Schu S4 (fig. 2–1 in Anno *et al.*, 1998).

near-maximum body temperature for high fever (T_h in °F) is determined as the first temperature value after onset that is followed by three lower values. The rise time for high fever (Δ_t in days) is defined as the time interval from fever onset until the time (t_h in days) at which the near-maximum body temperature is reached.

Table II. Parameters for the Lognormal Dose–Response Function for the Probability of Illness

Endpoint/Parameter	Values (95% Confidence Interval)
*ED*10	2.1 (0.1, 15.2)
*ED*50	9.8 (2.0, 27.1)
*ED*90	45 (22, 217)
α	–1.910
β	0.8376
μ	2.2803
σ	1.1939

Note: Summarized from Anno et al. (1998), which provides additional information on parameter uncertainties.

2.2. Mathematical Models

This subsection describes the mathematical methods used to develop a disease incidence model, a statistical characterization of the early fever profile among the Operation Whitecoat volunteers, and a stochastic model of the early fever profile for tularemia.

2.2.1. Disease Incidence Model

The data for incidence of tularemia (febrile illness or no febrile illness) for 118 unvaccinated subjects as compiled from Operation Whitecoat and analyzed by Anno et al. (1998) are listed in Table I. Illness is determined by the criterion described above

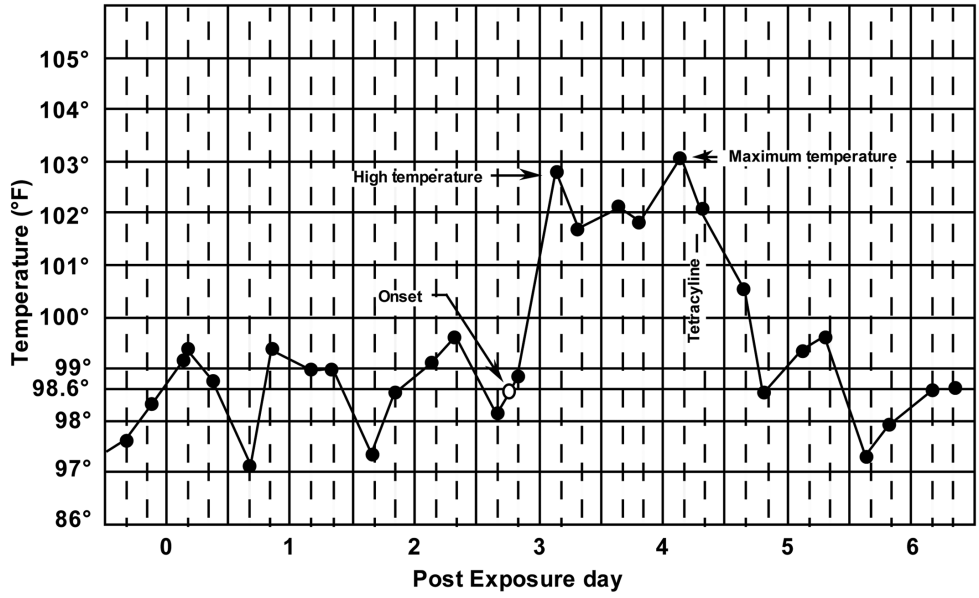

Fig. 4. Clinical record body temperature chart redrawn from actual clinical record for human volunteer administered aerosolized *F. tularensis* strain Schu S4 (fig. 2–5 in Anno et al., 1998).

for febrile illness following individual inhaled doses from 10 to 62,000 *F. tularensis* organisms. The reported unit of measure for doses is "organisms." To retain fidelity in the interpretation of the original data, the term "organisms" will be used throughout this article. However, the term in this context is considered equivalent to viable organisms or the more usual "colony forming units (CFUs)." For inhaled doses ≥46 organisms, all subjects became ill (101 of 118 volunteers documented in Table I). Anno *et al.* obtained empirical dose–response relationships for a subset of the data, excluding the doses above 400 organisms that caused 100% illness. The data for doses below 400 organisms (first 26 doses in Table I) were analyzed using maximum likelihood analysis for multiple forms of the probit model (normal, lognormal, Weibull, logistic, and log-logistic). The lognormal and log-logistic models best described the data. The lognormal model was carried forward in subsequent analyses by DTRA and OTSG and is the basis of this work.

Let N be the integer number of organisms inhaled by an individual in a population whose members are all exposed to the same aerosol environment. Because of randomness in the environment (such as air turbulence) and randomness among individuals (such as breathing rate and nasal geometry), there will be variation in N across the population. Let the mean number of inhaled organisms (averaged over the population) be $n = < N >$, where $0 \le n \le \infty$. The lognormal form of the dose–response function assumes that the incidence of febrile illness in the population is given by the cumulative normal distribution of the logarithm of the mean inhaled number of organisms. (We follow Anno et al. in using the natural logarithm as the dose parameter $d = \ln(n)$.) With these assumptions, the incidence of illness is given by the probability function $\Phi(d)$:

$$\Phi(d) = \left(\sqrt{2\pi}\sigma\right)^{-1} \int_{-\infty}^{d} \exp\left[-\frac{1}{2}\left(\frac{x-\mu}{\sigma}\right)^2 \frac{a+b}{c}\right] dx, \quad d = \ln(n)$$

$$= \frac{1}{2}\left[1 + \operatorname{erf}\left(\frac{d-\mu}{\sqrt{2}\sigma}\right)\right], \quad -\infty \le d \le \infty,\ 0 \le \Phi \le 1,$$

where μ and σ are the mean and standard deviation of the lognormal distribution, respectively. Hence, μ is the logarithm of the median effective dose, that is, the logarithm of the dose causing illness in half the exposed population. The probit slope of the lognormal distribution is σ^{-1}. Defining new variables α and β such that

$$\alpha = -\frac{\mu}{\sigma}, \quad \beta = \frac{1}{\sigma},$$

$$\mu = -\frac{\alpha}{\beta}, \quad \sigma = \frac{1}{\beta}$$

gives an alternative form of the incidence of febrile illness:

$$\Phi(d) = \frac{1}{2}\left[1 + \operatorname{erf}\left(\frac{\alpha + \beta d}{\sqrt{2}}\right)\right],$$

where α and β are the probit parameters derived by maximum likelihood analyses of the quantal response data. Table II presents values for these parameters.

It is important to remember that the organism doses listed in Table I are estimated from experimental conditions rather than being an actual count of inhaled organisms. Therefore, in terms of the variables defined above, the listed doses are values of n rather than N. With this in mind, the lognormal dose–response function $\Phi(d)$ serves as either the incidence of illness in a population or the probability that an individual will become ill.

2.2.2. *Statistical Characterization of the Early Fever Profile*

Dose-dependent parameter relationships for the 112 febrile volunteers were developed based on linear regression models for various transformations of the following three parameters:

$t_0 =$ IP (or onset time) relative to time of exposure (days)
$T_h =$ near-maximum body temperature (°F)
$\Delta_t =$ rise time, the interval between onset and reaching near-maximum body temperature (days)

A set of regression models for t_0, T_h, and Δ_t was developed that led to dose-parameterized probability distributions for these three quantities. These models may be used for Monte Carlo simulation of the distribution of body temperature across the individuals in an exposed population, parameterized by time after exposure and dose.

The general form of the regression models for parameter X_i as a function of dose n,

$$X_i = a_i + b_i \ln(n) + \varepsilon_i,$$

is a linear function of the natural logarithm of the dose with intercept, slope b_i, and a random contribution ε_i to be determined through maximum likelihood analysis. The X_i are related to t_0, T_h, and Δ_t by nonlinear transformations chosen to result in

normally distributed variables, either logarithmic or logistic. The time parameters themselves do not have Gaussian sampling distributions because they are constrained to be nonnegative. Similarly, the fever rise cannot be normally distributed because it must also be nonnegative and has an upper limit. Logarithmic and logistic transformations are used as described below so that the transformed quantities X_i may be reasonably assumed to be normal deviates for the purpose of simulation. In particular, it is assumed that the X_i are normally distributed as $X_i \sim N(a_i + b_i \ln(n), \sigma_i^2)$ and that the residuals $\varepsilon_i = X_i - (a_i + b_i \ln(n))$ are jointly distributed normal deviates with mean zero and standard deviation σ_i independent of $\ln(n)$. The parameters a_i, b_i, σ_i are taken to be their least-squares estimates $\hat{a}_i, \hat{b}_i, \hat{\sigma}_i$ and the linear equations $X_i = \hat{a}_i + \hat{b}_i \ln(n) + N(0, \hat{\sigma}_i^2)$ are used to generate random samplings of the quantities X_i.

The specific regression models used are based on the following definitions:

(i) $X_1 = \ln(t_0)$ is a Gaussian variate whose mean, μ_1, is a linear function of $\ln(n)$ and whose variance, σ_1^2, is independent of inhaled dose, n (i.e., homoscedasticity).
(ii) $X_2 = \ln(\Delta_t/(2.5 - \Delta_t))$, where $\Delta_t = t_h - t_0$ is a Gaussian variate whose mean, μ_2, is a linear function of $\ln(n)$ and whose variance, σ_2^2, is also independent of inhaled dose, n.
(iii) The variates X_1 and X_2 have a joint bivariate Gaussian distribution function entirely described by the four quantities, $\mu_1 = \mu_1(n)$, $\mu_2 = \mu_2(n)$, σ_1, and σ_2.
(iv) $X_3 = \ln((T_h - 100)/(106 - T_h))$ is a Gaussian variate whose mean, μ_3, is a linear function of $\ln(n)$ and whose variance, σ_3^2, is independent of inhaled dose, n. Furthermore, X_3 is presumed to be independent of X_1 and X_2 and may therefore be treated altogether separately.

Mathematically, these three definitions may be equivalently stated as:

(i) $X_1 = \ln(t_0) = a_1 + b_1 \ln(n) + \varepsilon_1$.
(ii) $X_2 = \ln(\Delta_t/(2.5 - \Delta_t)) = a_2 + b_2 \ln(n) + \varepsilon_2$, where ε_1 and ε_2 are joint Gaussian zero-mean variates with standard deviations σ_1 and σ_2 (both independent of inhaled dose). In practice, of course, the population parameters σ_1 and σ_2 must be replaced by reasonable estimators (i.e., their sampling statistics) that are byproducts of the usual regression procedure.
(iii) $X_3 = \ln((T_h - 100)/(106 - T_h)) = a_3 + b_3 \ln(n) + \varepsilon_3$, where ε_3 is a zero-mean Gaussian variate with standard deviation σ_3.

As consequences of these modeling assumptions, the following are guaranteed:

(i) $t_0 = \exp(X_1) > 0$, for all inhaled doses and all "draws" on the Gaussian variate X_1 (i.e., the entire range of values of the random variable t_0 consists of positive values).
(ii) $t_h - t_0 \equiv \Delta_t = 2.5/(1 + \exp(-X_2))$ for all inhaled doses and all "draws," that is, the entire range of values of the random variable $t_h - t_0$ consists of positive values. Hence, if first a value of $t_0 = \exp(X_1)$ is drawn and then a value of $\Delta_t = 2.5/(1 + \exp(-X_2))$, the value of $t_h = t_0 + \Delta_t$ will necessarily be greater than t_0. Furthermore, by virtue of the logistic form of X_2, the values of Δ_t obtained will be constrained to lie in the range $0 < \Delta_t < 2.5$ days, which is consistent with the two-part formula utilized above. $T_h = 100/(1 + \exp(X_3)) + 106/(1 + \exp(-X_3))$ is constrained to lie in the range $100\,^{\circ}\mathrm{F} < T_h < 106\,^{\circ}\mathrm{F}$ for all doses and all sample "draws" from the Gaussian variate X_3. The upper limit of 106 °F is a physiologically plausible maximal value. The lower limit of 100 °F is consistent with the definition of illness used to analyze the Operation Whitecoat data. The upper constraint of 2.5 days on the value of the fever rise time Δ_t is a judiciously chosen value greater than the maximum value of 2.3 days appearing in the data. Sensitivity to this value or to the chosen limits on the high temperature T_h was not investigated.

In the original analysis, Anno et al. (2005) tested for a correlation between the unexplained variance ε in the variates X_1 and X_2 but did not find one. They also verified homoscedasticity as defined above for X_1, X_2 and X_3. The Operation Whitecoat data fits corresponding to the linear regressions discussed above are described in Section 3.

2.2.3. Stochastic Model of Fever Profile and Application to Monte Carlo Simulation

Using the variables described above, Anno et al. (1998) model the time-dependent body temperature

$T(t)$ after onset of febrile illness with the following equation:

$$T(t) = 98.55 + \frac{T_m - 98.55}{1 + \left(\frac{T_m - T_0}{T_0 - 98.55}\right) e^{-k(t-t_0)}} \quad (t > t_0),$$

where normal body temperature is $T_0 = 98.6$ °F (the value at $t = t_0$) and the maximum body temperature approaches a value of T_m at late times ($t >> t_0$). This mathematical form allows the fever in the initial phase of illness to rise exponentially with a characteristic rate k after onset, but then level out at the maximum value T_m as illustrated in Fig. 1. This equation offers a reasonable analytic form to empirically describe the initial phase of illness. Anno et al. (1998) motivate this form by analogy with the similar mathematical form arising from the logistic equation for self-limiting bacterial growth first proposed by Verhulst (Verhulst, 1838). The value of 98.55 °F appearing in the equation is a judiciously chosen reference value that is a small increment $\Delta T_0 = 0.05$ °F below normal body temperature. Small in this context means that ΔT_0 is much smaller than the maximum fever rise $T_\mathrm{m} - T_0$.

We may find the value of k by using the high (i.e., near-maximum) temperature T_h defined above from the clinical data. This value is reached at a time $t_\mathrm{h} = t_0 + \Delta_\mathrm{t}$, so $T_\mathrm{h} = T(t_0 + \Delta_\mathrm{t})$. Using these expressions in the equation above and solving for k, we find:

$$k = {\Delta_t}^{-1} \ln\left(\frac{20\,(T_h - 98.55)\,(T_m - T_0)}{(T_m - T_h)}\right).$$

From the Operation Whitecoat data, Anno et al. (1998) estimated that $T_m - T_h \cong 0.17$ °F. An alternative approach to modeling the fever profile would be to estimate the parameters of the logistic equation directly from the Operation Whitecoat data.

The time profile of early-phase fever may be estimated from the values of the time of onset t_0, the near-maximum body temperature T_h, and the rise time after onset to reach near-maximum temperature, Δ_t. For an exposed population, random draws of these three parameters for each individual given his dose may be used to generate a stochastic simulation of the fever profile for each member of the population. Taken together these simulations constitute a Monte Carlo simulation of the response of the population. Criteria regarding consequences of the fever may be used to predict outcomes such as the patient stream resulting from exposure of a military unit as described in Section 3.3. Although such Monte Carlo simulations could be elaborated to account for model parameter uncertainties derived from the Operation Whitecoat data, simulations reported here are based on the central values of the parameters.

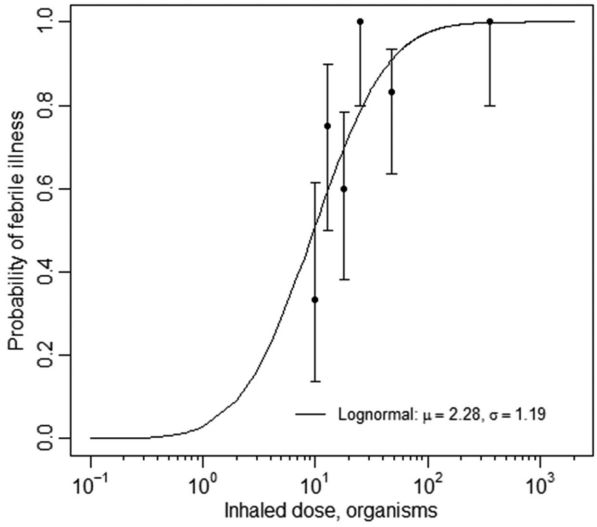

Fig. 5. Dose–response model for human tularemia by the inhalation route. The median effective dose (ED_{50}) is 9.8 organisms (or CFUs).

3. RESULTS

The Operation Whitecoat human data set for unvaccinated, healthy adult males informs generation of a model of the early phase of febrile illness associated with tularemia, which includes a dose–response model for illness and a stochastic model of early-phase fever (Fig. 2). The data for 112 febrile volunteers supports both time- and dose-dependent analysis using the model for the febrile illness profile (Fig. 4) described above with three parameters: IP (t_o); rise time for high fever (Δ_t); and near-maximum (high) temperature (T_h). All three of these characteristic parameters are subject to dose dependence and random variation from individual to individual. Analysis of these extensive human data provides well-founded mathematical descriptions of these parameters and their variability.

3.1. Dose–Response Model for Fever

The deterministic dose–response function is illustrated in Fig. 5 for the incidence of febrile illness associated with inhaled doses of *F. tularensis*. A lognormal dose–response function is fitted via maximum likelihood analysis to the human data from the 26 volunteers administered the lowest doses

(estimated inhaled doses 10–398 organisms; Table I), six of whom did not develop febrile illness.

The best fit parameters $\mu = 2.28$ and $\sigma = 1.19$ correspond to a median effective dose (ED_{50}) for febrile illness of 9.8 organisms for *F. tularensis* strain Schu S4, in agreement with the analysis reported by Anno et al. (1998), who cite a 95% confidence interval on the ED_{50} from 2.0 to 27, as shown in Table II. For display purposes in Fig. 5, the 26 data points are divided into six dose ranges: 1–10, 11–15, 16–20, 21–30, 31–60, and 61–400. The probability of response for each range is the average of the response (0 for no, 1 for yes) for the subjects in the range. The average response for each range is plotted at the geometric mean of the subject doses within the range. The error bars on the average response represent the 68% confidence interval band according to the Wilson score interval for a binomial distribution.

3.2. Regression Parameters for Initial Fever Profile

The data for the 112 volunteers who developed early-phase febrile illness (Table I) inform development of the regression models for the three fever profile parameters (t_o; Δ_t; T_h). The regression models for all three parameters provide reliable representations ($p < 10^{-6}$) of the fever profiles. Table III presents the regression parameters for the Gaussian variants determining the three fever profile parameters as described above.

The regression models for the dose-dependent fever parameters for early-phase illness are plotted in Figs. 6–8. The dots represent the actual observations for each of the 112 volunteers who developed febrile illness. The central curves represent the median response as a function of inhaled dose. At a given inhaled dose, individual variability about the median value is modeled with a dose-independent Gaussian variate as described above. The inner pair of curves represents the 95% confidence band for the median value of the dose-dependent parameters. The outer

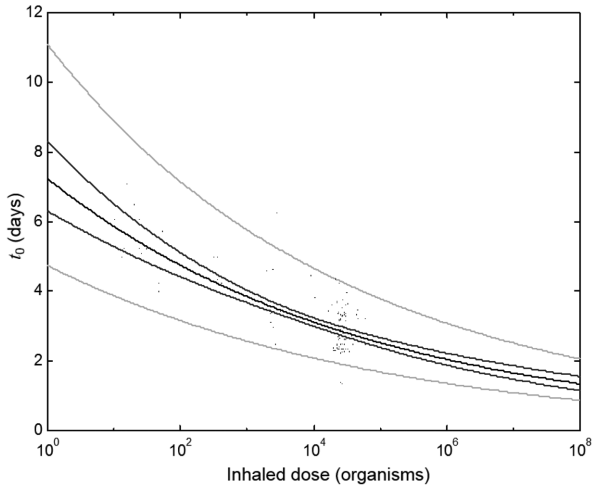

Fig. 6. Dose-dependent incubation period (onset time) of febrile illness in 112 human volunteers who developed tularemia after administration of aerosols of *F. tularensis* strain Schu S4 (fig. 5–16 in Anno et al., 2005).

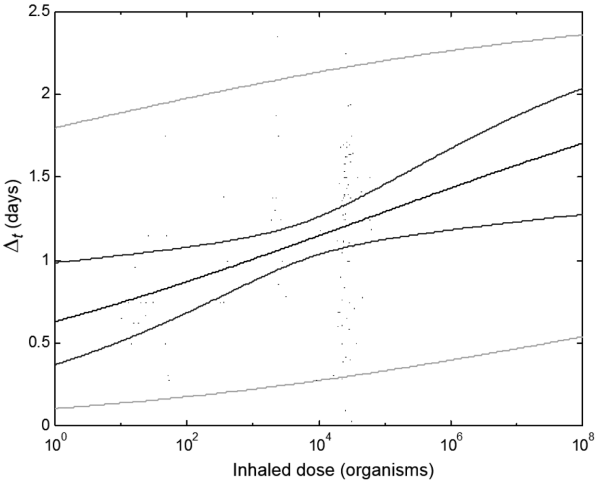

Fig. 7. Dose-dependent rise times to high (near-maximum) fever for early-phase tularemia in human volunteers administered aerosols of *F. tularensis* strain Schu S4 (fig. 5–17 in Anno et al., 2005).

Table III. Regression Parameters for the Gaussian Variants Determining the Three Fever Profile Parameters

	Coefficients		Coefficient Error Statistics			Estimator of σ
Variate	a	b	$\sigma_{\mathbf{a}}$	$\sigma_{\mathbf{b}}$	Cov(a,b)	S_{yx}
$X_1 = \ln(t_0)$	1.981	–0.091	0.070	0.008	–0.00052	0.2048
$X_2 = \ln(\frac{\Delta_t}{2.5-\Delta_t})$	–1.092	0.101	0.337	0.037	–0.01192	0.9826
$X_3 = \ln(\frac{T_h-100}{106-T_h})$	–1.332	0.162	0.257	0.028	–0.00694	0.7495

Note: Summarized from Anno et al. (2005), which provides additional information on parameter uncertainties.

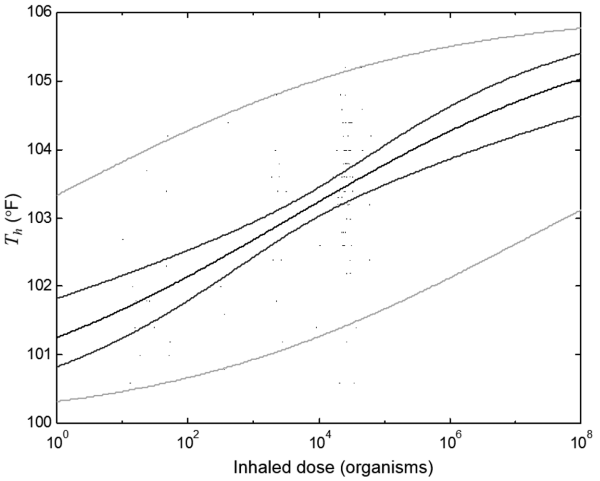

Fig. 8. Logistic model for dose-dependent near-maximum body temperature as a function of inhaled dose (fig. 5–19 in Anno et al., 2005).

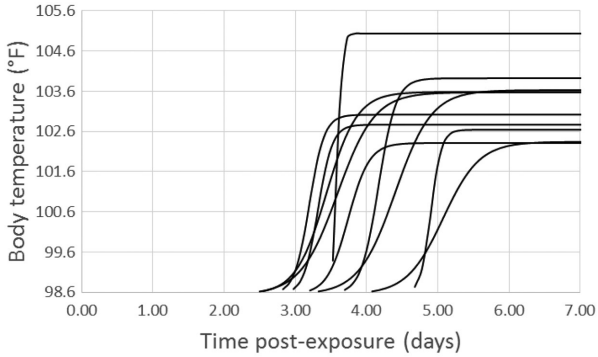

Fig. 9. Stochastic simulation of the early-phase fever profiles for 10 individuals with tularemia after an inhaled dose of 5,000 organisms, mean inhaled dose.

pair of curves represents the 95% confidence region for predictions of single simulated observations, as a function of inhaled dose, based on the distribution of parameters for the febrile volunteers.

The results for the IP (relative to exposure) are illustrated in Fig. 6. The central curve is the median onset time as a function of inhaled dose. The inner pair of curves represents the 95% confidence band for the mean value of the dose-dependent onset time. The outer pair of curves represents the 95% confidence region for predictions of single simulated observations, as a function of inhaled dose, based on the distribution of incubation times for volunteers. Note that variability in IP is higher at lower doses, with prediction intervals ranging from 4–10 days at the lowest dose tested and 2–5 days at the highest dose tested.

The fever rise time model is illustrated in Fig. 7. The analysis is based on the same logistic function as used for the near-maximum temperature. In this case, the possible range of values is assumed to be limited to between 0 and 2.5 days. As in the previous figure, Fig. 7 includes the actual data points for fever rise time for each febrile subject, the dose-dependent median curve and its 95% confidence band, as well as the pair of outer curves giving the 95% confidence band for prediction intervals for single observations of rise time as a function of inhaled dose. Note that as inhaled dose increases (Fig. 7), so does the time to reach the maximum temperature (rise time). While the time to onset decreases with increasing inhaled dose (Fig. 6), there is a trend of increasing time required to reach the near-maximum temperature (rise time; Fig. 7). Though this may seem counterintuitive, time is required physiologically to raise body temperature. It appears from these data that the higher the temperature, the longer the time required to reach that higher temperature. Note that variability in rise time does not appear to increase markedly with decreasing dose.

The near-maximum body temperature model for those 112 volunteers who became ill is illustrated in Fig. 8. Note that the minimum value for the near-maximum temperature is 100 °F by definition. In the analysis, it is assumed that the body temperature could not go above 106 °F. A logistic function is applied to the data to transform the resulting 6 °F range to a variable ranging from $-\infty$ to $+\infty$ in order to perform a standard linear regression on the data. As in the two previous figures, Fig. 8 displays the actual data for near-maximum temperature as dots corresponding to each febrile subject, the dose-dependent median curve and its 95% confidence band, as well as the outer pair of curves giving the 95% confidence band for the prediction intervals for single observations of near-maximum temperature as a function of inhaled dose. Note that variability in near-maximum body temperature does not appear to increase markedly with decreasing dose.

3.3. Application of the Stochastic Fever Profile Model

Simulations of illness using the stochastic fever profile model for the same inhaled dose (5,000 organisms) for a group of 10 individuals are illustrated

in Fig. 9. The figure shows onset of illness ranging from 2.5 to 4.5 days and a maximum fever ranging from 102 to 105 °F among the 10 individuals. The individual variations in IP, fever rise time, and peak fever are not correlated at a given dose and so are drawn as independent variates from the distributions described above for the Operation Whitecoat data. The individual-to-individual degree of fever varies even when all receive the same dose (Fig. 9). A similar procedure may be followed for the more realistic situation where meteorology and location of troops results in a wide range of doses encountered by each individual. In this case, the varying dose from individual to individual would result in even more variation in fever profiles than shown by Fig. 9.

Stochastic simulations using the model of early-phase illness for pneumonic tularemia illustrated in Fig. 9 can be used to make Monte Carlo predictions of the patient stream for routine and combat situations. In these two situations, the degree of fever that causes an individual to seek medical care may differ. The left-hand column of three panels in Fig. 10 provides a Monte Carlo simulation of the response of a company-sized unit (90 individuals) given a dose of 10 organisms to each individual soldier. The histograms show times after exposure for three different patient conditions: (1) time of onset of fever, (2) time for sufficient signs and symptoms to cause the individual to seek medical care under routine operations (though he would be capable of continued duty if so required), and (3) time for sufficient progression of illness for the individual to become a litter patient (or, stated differently, to become an operational casualty unable to perform in a combat or other emergency situation). For the illustration in Fig. 10, the second condition (seek medical care) is assumed to occur when fever reaches 101.4 °F and the third condition (litter patient) is assumed to occur when fever reaches 104.2 °F. These values are based on performance degradation of 25% and 75%, respectively, estimated (Anno et al., 1998) for tasks involving short-term endurance and may vary from one scenario to another.

Panels (a)–(c) in Fig. 10 correspond to a uniform inhaled dose equal to the median effective dose for *F. tularensis*. The Monte Carlo simulation of the company results in 41 of 90 individuals experiencing an onset of fever. Of these 41, 30 seek medical care, and 9 become litter patients during the early phase of illness in the absence of treatment. The set of histograms shown in panels (d)–(f) of Fig. 10 correspond to a uniform inhaled dose of 10,000 organisms. At this higher dose, all 90 individuals experience the onset of fever with 86 seeking medical care, and 56 becoming litter patients in the absence of treatment. The distributions of onset time and time to seek medical care occur about two days earlier than for the lower dose in the left-hand panels. The variability of these two times from person to person for the higher dose is also reduced, decreasing from a spread of about four days at the lower dose to about two days for the higher. It is worth noting that these estimates at the higher dose are not extrapolations. The majority of the human volunteers on which the simulations are based had even higher doses (see Table I).

4. DISCUSSION

The statistical characterization of the complete data set from 118 volunteers (112 febrile with measured IP, fever rise time, and near-maximum fever) fills gaps in knowledge about early-phase human tularemia unappreciated in previously published studies from portions of these data (Egan, Hall, & Leach, 2011; Jones, Nicas, Hubbard, Sylvester, & Reingold, 2005; Wood, Egan, & Hall, 2014). The statistical characterization of three parameters defining human fever profile are useful for comparisons to outputs of theoretical models of tularemia mechanisms, particularly IPs in animal models (Gillard, Laws, Lythe, & Molina-París, 2014; Huang & Haas, 2011; Wood et al., 2014) and from human epidemiologic investigation (Egan et al., 2011). All of these studies considered *F. tularensis* strain Schu S4. Although the study of Jones et al. (2005) did not consider temporal patterns for tularemia, this study is mentioned herein for completeness.

Egan et al. (2011) considered IP distributions based on both dose-dependent and dose-independent data (their fig. 2). Their dose-dependent IP distribution is generally consistent with the current study, as might be expected since the human data used by both groups overlap. However, a two-parameter probit dose–response model was selected in the current study over the simpler one-parameter exponential model of Egan et al. (2011) because this two-parameter model provides good fits to both naïve (Fig. 5) and vaccinated (Fig. 11) volunteers. The ED_{50} for the exponential model is determined entirely by the probability p_1 that a single inhaled organism will cause fever. As illustrated in Fig. 11, the exponential model will not accommodate the variability in immune response of the vaccinated human volunteers (Anno et al., 1998) as does the adjustable

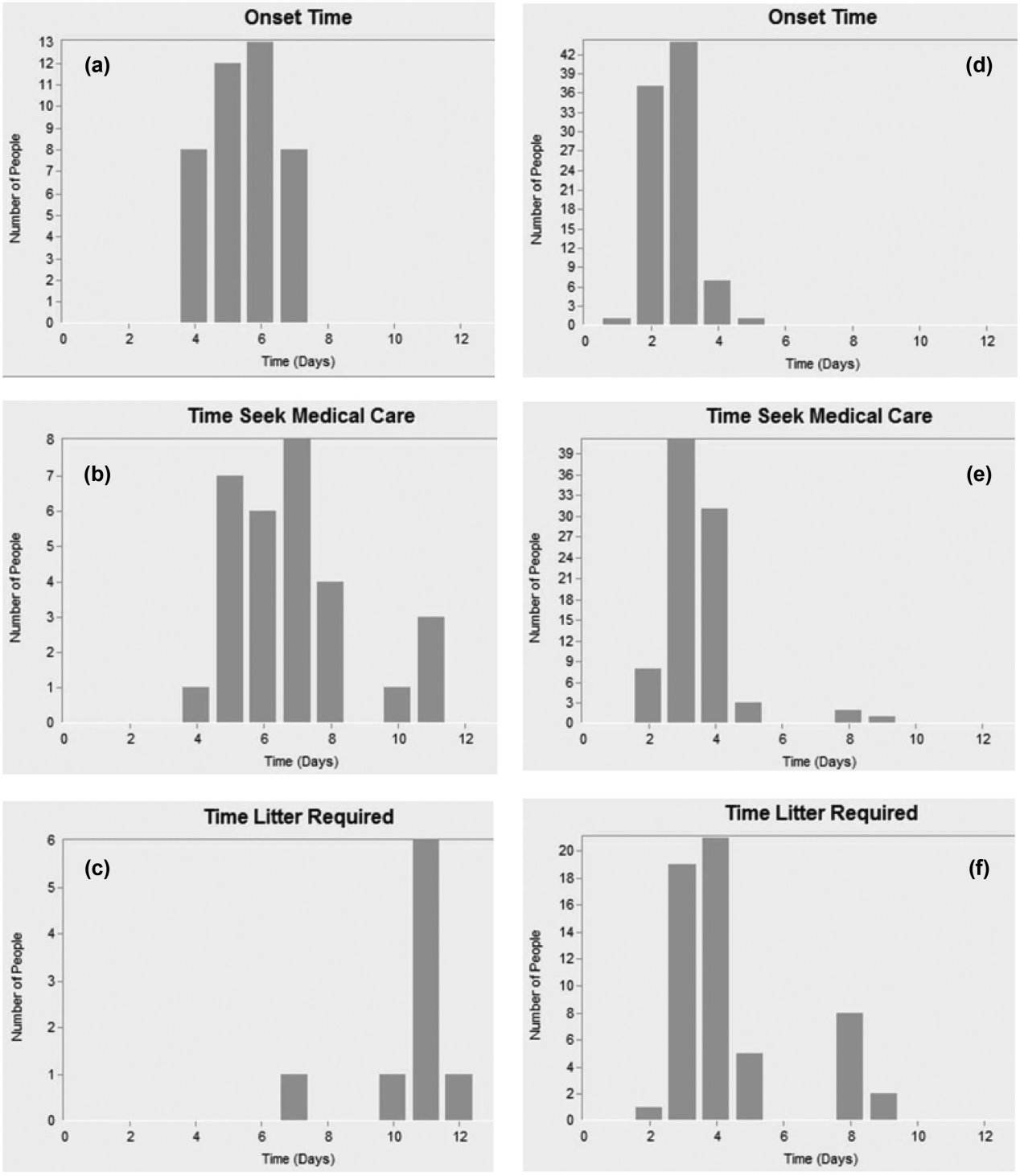

Fig. 10. Monte Carlo simulation of patient streams for two exposure levels for a company-sized unit (90 individuals): 10 organisms, mean inhaled dose (a), (b), and (c); and 10,000 organisms, mean inhaled dose (d), (e), and (f).

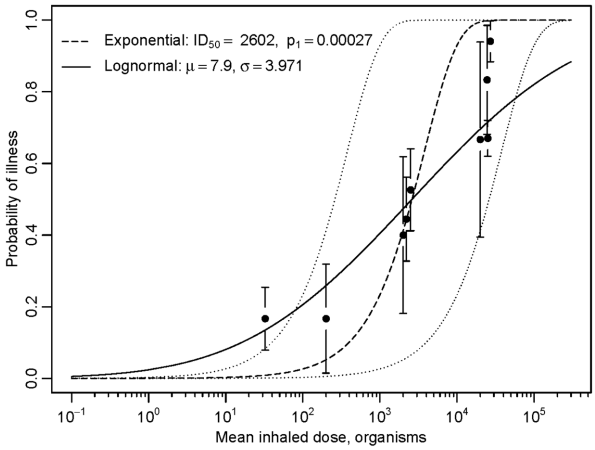

Fig. 11. The lognormal model accommodates population variability by fitting the slope of dose–response data for vaccinated individuals (Anno et al., 1998) that cannot be accommodated by the exponential model.

slope of the two-parameter lognormal model. For illustration, three parallel curves for the exponential model are plotted in Fig. 11. The central, dashed curve is drawn for a value of p_1 yielding the same ED_{50} as the best-fit lognormal curve (solid curve). With no other parameter to adjust, the exponential model predicts the same value of the slope at the ED_{50} for any value of the ED_{50}, as illustrated by the two parallel dotted curves in Fig. 11. These parallel curves correspond to ED_{50} values a factor of 10 lower and higher for illustration. Because of the discrepancy in predicted slope, attempted maximum likelihood fits of the exponential model to the data for the vaccinated individuals would not converge. Other two-parameter models, including the beta-Poisson model (Haas, 2015), could be considered in addition to the lognormal model for disease incidence with and without immunity.

Two dose–response analyses in the literature considered only data from animal models. Huang and Haas (2011) described fitting an exponential dose–response model and incorporating time to death based on data from a Rhesus monkey study that administered aerosols of *F. tularensis* of various organism number mean diameters from 2.1 to 24 μm. Note that the beta Poisson model did not provide a statistically significant improvement in fit over the exponential model. Gillard et al. (2014) described theoretical mechanisms for tularemia progression in BALB/c mice administered 100 CFU by aerosol or nasopharyngeal routes for the first 48 hours of pathogenesis. Knowledge of the nature and magnitude of mechanisms driving pathogenesis in humans, nonhuman primates, and murine species would be needed for interspecies extrapolation of such modeling results in human health risk assessments.

The major strengths of this study for informing military decisionmakers about the operational risks of pneumonic tularemia are that: (1) the data set is based on human subjects, specifically, 118 naïve (unvaccinated) volunteers; (2) human fever endpoints are available in the early phase of illness (prior to antibiotic administration) for the 112 volunteers who became ill; and (3) the mathematical model provides a time- and dose-dependent statistical characterization of multiple responses (i.e., IP, high-fever degree, and rise time to high fever). The low-dose data determine the dose–response curve for incidence of febrile illness for this highly infectious agent, and the data set for the 112 febrile volunteers provides a statistical description of the progression of illness as functions of dose and time.

This detailed description of health status over time for exposed troops is important in an operational context to understand the risks over time to mission effectiveness posed by intentional exposures to *F. tularensis* in a biological attack. For example, although the pathogen causes illness at low doses ($ED_{50(\text{fever})} = 9.8$ inhaled organisms), these low doses are associated with IPs and times to high fever of nearly a week, potentially giving time to complete an operation and then provide prophylactic treatment to prevent clinical illness. Even after high inhaled doses, illness is unlikely for two or more days (Fig. 6), and antibiotic treatment typically clears fever within one or two days without recurrence or chronic effects. From a medical planning viewpoint for a given attack on a military unit or a population, the mathematical model predicts the time distribution of the number of individuals seeking medical care, thereby providing an estimate of the patient stream to be handled by medical treatment facilities.

Due to well-documented differences in strain infectivity and virulence (Eigelsbach & Hornick, 1973; Schricker, Eigelsbach, Mitten, & Hall, 1972; World Health Organization, 2007), exposures to endemic strains of *F. tularensis* may or may not result in clinical disease patterns observed in Operation Whitecoat volunteers exposed to the highly infectious strain Schu S4. It is possible, however, to modify the statistical parameters of the model to describe other strains when appropriate data are available. Finally, the model described herein may be adapted to other biological agents causing early-phase febrile illness.

5. CONCLUSIONS

The data set for inhalation-induced tularemia generated in Operation Whitecoat confirms that *F. tularensis* strain Schu S4 is highly infectious ($ED_{50(\text{fever})}$ of about 10 organisms inhaled) and characterizes early-phase febrile illness parameters that are both dose- and time-dependent (IP, near-maximum temperature, and rise time). Based on the statistical characterization of early-phase fever in the human volunteers, the model provides reliable insight into the health and operational readiness of exposed troops and other personnel for as long as one week after exposure. For longer times, the model is less certain and requires additional information for modeling later-phase illness.

ACKNOWLEDGMENTS

Funding for the first U.S. government technical report authored by Anno et al. (2005) and cited herein was provided by the Defense Special Weapons Agency, Alexandria, VA to better understand biological agent threats. Funding for the second U.S. government technical report authored by Anno et al. (1998) and cited herein was provided by the U.S. Army Office of the Surgeon General, Health Care Operations (DASG-HCO) to support publication by the North American Treaty Organization (NATO) of Allied Medical Publication 8(B), *Volume II, Medical Planning Guide of CBRN Battle Casualties (Biological)*. Portions of the two technical reports are used herein with only limited paraphrasing. The authors wish to recognize Mr. Ronald Bloom for much of the statistical analyses drawn from those reports. Bacteriological review of the analysis of Anno et al. (2005, 1998) was provided by the Walter Reed Army Institute of Research. Application of these data is part of the Army Public Health Center (APHC) project aimed at deriving exposure guidelines for biological agents of interest. The authors are grateful to Mr. Matthew McAtee, Mr. Stephen Comaty, and Dr. Gabriel Intano of APHC for many useful discussions and support.

The views expressed herein are those of the authors and do not necessarily reflect official policy of the U.S. Department of Defense, Department of the Army, or Army Medical Department, or of the U.S. Government. According to previous reports on which this study is based, human volunteer studies were initiated in conformity with the ethical principles recorded in Army Chief of Staff Memo Cs-385 (30 June 1953) and Army Regulation 70-25 (26 March 1962).

The authors dedicate this article to the memory of the late George H. Anno (1930-2014) who was the visionary driving force behind the models and analyses reported herein.

REFERENCES

Adamovicz, J., Wargo, E., & Waag, D. (2006). Chapter 9: Tularemia. In J. R. Swearengen (Ed.), *Biodefense research methodology and animal models*. New York: Taylor & Francis.

Alluisi, E. A., Beisel, W. R., Bartelloni, P. J., & Coates, G. D. (1973). Behavioral effects of tularemia and sandfly fever in man. *Journal of Infectious Diseases*, *128*(6), 710–717.

Anno, G. H., Lockhart, M., Karns, L., McClellan, G. E., Rickmeier, G. L., Bloom, R. N., & Matheson, L. N. (2005). Biological agent exposure and casualty estimation: AMedP-8 (biological) methods report. Falls Church, VA: U.S. Army Office of the Surgeon General Technical Report for Contract No. GS-35F-4923H.

Anno, G. H., Sanenitsu, S. K., McClellan, G. E., Dore, M. A., & Deverill, A. P. (1998). Consequence analytic tools for NBC operations volume 1: Biological agent effects and degraded personnel performance for tularemia, staphylococcal enterotoxin B (SEB) and Q fever. Defense Special Weapons Agency, Alexandria, VADSWA-TR-97-61-V1.

Barry, M. (2005). Report of pneumonic tularemia in three Boston University researchers: Boston Public Health Commission. November 2004–March. Retrieved from: https://www.cbc.arizona.edu/sites/default/files/Boston_University_Tularemia_report_2005.pdf.

Burke, D. S. (1977). Immunization against tularemia: Analysis of the effectiveness of live Francisella tularensis vaccine in prevention of laboratory-acquired tularemia. *Journal of Infectious Diseases*, *135*(1), 55–60.

Centers for Disease Control and Prevention (CDC). (2002). Tularemia—United States, 1990–2000. *MMWR Morbidity and Mortality Weekly Report*, *51*(9), 181.

Centers for Disease Control and Prevention (CDC). (2003). Tularemia fact sheet. Retrieved from: https://www.bt.cdc.gov/agent/tularemia/faq.asp.

Centers for Disease Control and Prevention (CDC). (2017). Federal select agent program: Select agents and toxins list. Retrieved from: https://www.selectagents.gov/SelectAgentsandToxinsList.html.

Dahlstrand, S., Ringertz, O., & Zetterberg, B. (1971). Airborne tularemia in Sweden. *Scandinavian Journal of Infectious Diseases*, *3*(1), 7–16.

Dembek, Z. F. (2007). Tularemia. In *Medical management of biological casualties handbook*. Office of the Surgeon General, U.S. Army. Washington, DC: Borden Institute: Walter Reed Medical Center.

Dembek, Z. F., Pavlin, M., & Kortepeter, M. G. (2007). Epidemiology of biowarfare and bioterrorism. In *Textbook of military medicine: Medical aspects of biological warfare*. Washington, DC: TMM Publications, Borden Institute, Walter Reed Army Medical Center, 39–68.

Dempsey, M. P., Nietfeldt, J., Ravel, J., Hinrichs, S., Crawford, R., & Benson, A. K. (2006). Paired-end sequence mapping detects extensive genomic rearrangement and translocation during divergence of Francisella tularensis subsp. tularensis and Francisella tularensis subsp. holarctica populations. *Journal of Bacteriology*, *188*(16), 5904–5914.

Egan, J. R., Hall, I. M., & Leach, S. (2011). Modeling inhalational tularemia: Deliberate release and public health response.

Biosecurity and Bioterrorism: Biodefense Strategy, Practice, and Science, *9*(4), 331–343.
Eigelsbach, H., & Hornick, R. (1973). Continued studies on aerogenic immunization of man with live tularemia vaccine. In *Airborne transmission and airborne infection*. Utrecht, The Netherlands: Oosthoeck Publishing Co. 319–22.
Eigelsbach H., Saslaw S., Tulis J., & Hornick R. (Eds.) (1968). *Tularemia: The monkey as a model for man. Use of nonhuman primates in drug evaluation, a symposium*. San Antonio, TX: Southwestern Foundation for Research and Education.
Eigelsbach, H., Tigertt, W., Saslaw, S., & McCrumb, Jr F. (Eds.) (1962). *Live and killed tularemia vaccines: Evaluation in animals and man*. Proceedings of the 1962 Army Science Conference, U.S. Army Military Academy, West Point, NY.
Eliasson, H., Lindbäck, J., Nuorti, J. P., Arneborn, M., Giesecke, J., & Tegnell, A. (2002). The 2000 tularemia outbreak: A case-control study of risk factors in disease-endemic and emergent areas, Sweden. *Emerging Infectious Diseases*, *8*(9), 956.
Feldman, K. A., Enscore, R. E., Lathrop, S. L., Matyas, B. T., McGuill, M., Schriefer, M. E., … Hayes, B. E. (2001). An outbreak of primary pneumonic tularemia on Martha's Vineyard. *New England Journal of Medicine*, *345*(22), 1601–1606.
Gillard, J. J., Laws, T. R., Lythe, G., & Molina-París, C. (2014). Modeling early events in Francisella tularensis pathogenesis. *Frontiers in Cellular and Infection Microbiology*, *4*, 169.
Haas, C. N. (2015). Microbial dose response modeling: Past, present, and future. *Environmental Science & Technology*, *49*(3), 1245–1259.
Halsted, C. C., & Kulasinghe, H. P. (1978). Tularemia pneumonia in urban children. *Pediatrics*, *61*(4), 660–662.
Hauri, A. M., Hofstetter, I., Seibold, E., Kaysser, P., Eckert, J., Neubauer, H., … Splettstoesser, W. D. (2010). Investigating an airborne tularemia outbreak, Germany. *Emerging Infectious Diseases*, *16*(2), 238.
Hepburn, M., Friedlander, A., & Dembek, Z. (2007). Chapter 8: Tularemia. In Z. F. Dembek (Ed.), *Medical aspects of biological warfare*. Washington, DC: Borden Institute: Walter Reed Medical Center.
Hornick, R. B., & Eigelsbach, H. T. (1966). Aerogenic immunization of man with live Tularemia vaccine. *Bacteriological Reviews*, *30*(3), 532.
Huang, Y., & Haas, C. N. (2011). Quantification of the relationship between bacterial kinetics and host response for monkeys exposed to aerosolized Francisella tularensis. *Applied and Environmental Microbiology*, *77*(2), 485–490.
Hughes, W. T. (1963). Tularemia in children. *Journal of Pediatrics*, *62*(4), 495–502.
Jones, R. M., Nicas, M., Hubbard, A., Sylvester, M. D., & Reingold, A. (2005). The infectious dose of Francisella tularensis (tularemia). *Applied Biosafety*, *10*(4), 227–239.
Kaye, D. (2005). Tularemia, laboratory acquired, 1 March News *CID*, *40*(5), pages iii–iv.
Lyons, R. C., & Wu, T. H. (2007). Animal models of Francisella tularensis infection. *Annals of the New York Academy of Sciences*, *1105*(1), 238–265.
Martone, W. J., Marshall, L. W., Kaufmann, A. F., Hobbs, J. H., & Levy, M. E. (1979). Tularemia pneumonia in Washington, DC: A report of three cases with possible common-source exposures. *JAMA*, *242*(21), 2315–2317.
North Atlantic Treaty Organization. (2007). AMedP-8(B). In *Volume II: Medical planning guide for the estimation of CBRN battle casualties (biological)*.
Overholt, E. L., Tigertt, W., Kadull, P. J., Ward, M. K., David, C. N., Rene, R. M., … Stephens, M. (1961). An analysis of forty-two cases of laboratory-acquired tularemia: Treatment with broad spectrum antibiotics. *American Journal of Medicine*, *30*(5), 785–806.
Pekarek, R., Bostian, K., Bartelloni, P., Calia, F., & Beisel, W. (1969). The effects of Francisella tularensis infection on iron metabolism in man. *American Journal of the Medical Sciences*, *258*(1), 14–25.
Rusnak, J. M., Kortepeter, M. G., Hawley, R. J., Anderson, A. O., Boudreau, E., & Eitzen, E. (2004). Risk of occupationally acquired illnesses from biological threat agents in unvaccinated laboratory workers. *Biosecurity and Bioterrorism: Biodefense Strategy, Practice, and Science*, *2*(4), 281–293.
Saslaw, S., & Carhart, S. (1961). Studies with tularemia vaccines in volunteers. III. Serologie aspects following intracutaneous or respiratory challenge in both vaccinated and nonvaccinated volunteers. *American Journal of Medical Sciences*, *241*(6), 689–699.
Saslaw, S., Eigelsbach, H. T., Prior, J. A., Wilson, H. E., & Carhart, S. (1961). Tularemia vaccine study: II. Respiratory challenge. *Archives of Internal Medicine*, *107*(5), 702–714.
Sawyer, W. D., Dangerfield, H. G., Hogge, A. L., & Crozier, D. (1966). Antibiotic prophylaxis and therapy of airborne tularemia. *Bacteriological Reviews*, *30*(3), 542.
Schricker, R. L., Eigelsbach, H. T., Mitten, J. Q., & Hall, W. C. (1972). Pathogenesis of tularemia in monkeys aerogenically exposed to Francisella tularensis 425. *Infection and Immunity*, *5*(5), 734–744.
Shambaugh III, G. E., & Beisel, W. R. (1967). Early alterations in thyroid hormone physiology during acute infection in man. *Journal of Clinical Endocrinology & Metabolism*, *27*(12), 1667–1673.
Shapiro, D. S., & Schwartz, D. R. (2002). Exposure of laboratory workers to Francisella tularensis despite a bioterrorism procedure. *Journal of Clinical Microbiology*, *40*(6), 2278–2281.
Simpson, W. M. (1929). Tularemia: History. In *Pathology, diagnosis and treatment*. New York: Hoeber.
Sinclair, R., Boone, S. A., Greenberg, D., Keim, P., & Gerba, C. P. (2008). Persistence of category A select agents in the environment. *Applied and Environmental Microbiology*, *74*(3), 555–563.
Siret, V., Barataud, D., Prat, M., Vaillant, V., Ansart, S., Le Coustumier, A., … Capek, I. (2005). An outbreak of airborne tularaemia in France, August 2004. *Euro surveillance: Bulletin Europeen sur les maladies transmissibles = European Communicable Disease Bulletin*, *11*(2), 58–60.
Sunderrajan, E. V., Hutton, J., & Marienfeld, R. D. (1985). Adult respiratory distress syndrome secondary to tularemia pneumonia. *Archives of Internal Medicine*, *145*(8), 1435–1437.
Syrjälä, H., Kujala, P., Myllylä, V., & Salminen, A. (1985). Airborne transmission of tularemia in farmers. *Scandinavian Journal of Infectious Diseases*, *17*(4), 371–375.
USAMRIID. (2009). Update on USAMRIID scientist with tularemia. Retrieved from: https://www.usamriid.army.mil/press_releases/Tularemia%20News%20Rel%202.pdf.
USAMRIID. (2010). Tularemia in a laboratory worker at USAMRIID: Executive summary—April. Retrieved from: https://www.fredericknewspost.com/media/pdfs/tularemia-executive-summary.pdf.
Verhulst, P. -F. (1838). Notice sur la loi que la population suit dans son accroissement. *Correspondance Mathématique et Physique Publiée par a. Quetelet*, *10*, 113–121.
Weinstein, R. S., & Alibek, K. (2003). *Biological and chemical terrorism: A guide for healthcare providers and first responders*. New York: Thieme Medical Pub.
Wood, R., Egan, J., & Hall, I. (2014). A dose and time response Markov model for the in-host dynamics of infection with intracellular bacteria following inhalation: With application to Francisella tularensis. *Journal of the Royal Society Interface*, *11*(95), 20140119.
World Health Organization. (2007). *WHO guidelines on tularemia*. Geneva: World Health Organization. Retrieved from: https://www.cdc.gov/tularemia/resources/whotularemiamanual.pdf.